Hindawi
Journal of Food Biochemistry
Volume 2024, Article ID 6696954, 14 pages
https://doi.org/10.1155/2024/6696954

Research Article

Application of the Effect of Nonthermal Technologies on the Oxidation of Proteins and Lipids in Pigeon Meat during Chilled Storage

Xiao-Yang Tong,[1,2] Yi Zhang,[1] Jin-Xin Pang,[1] Bao-Lin Liu,[2] Eric Biron,[3] Md R. T. Rahman,[3] Yong-Jin Qiao,[1] Qi-Jie Bing,[4] and Xu-Ying Gao[5]

[1]*Research Center for Agricultural Products Preservation and Processing, Crop Breeding & Cultivation Research Institute, Shanghai Academy of Agricultural Sciences, Shanghai 201403, China*
[2]*School of Health Science and Engineering, University of Shanghai for Science and Technology, Shanghai 200093, China*
[3]*CHU de Québec Research Center, Université Laval, Québec, QC G1V 0A6, Canada*
[4]*Shanghai Mantou Tuna International Trade Co., Ltd., Shanghai 200433, China*
[5]*Shanghai Yihao Foods Co., Ltd., Shanghai 201400, China*

Correspondence should be addressed to Yi Zhang; 554114360@qq.com and Yong-Jin Qiao; qiaoyongjin@hotmail.com

Received 21 August 2023; Revised 23 November 2023; Accepted 26 March 2024; Published 4 April 2024

Academic Editor: Hongju He

This study investigated the effects of low-voltage electrostatic field (LVEF), electron beam irradiation (EBI), and modified atmosphere packaging (MAP) on protein and lipid oxidation of pigeon meat (PM) during chilled storage. The water-holding capacity (WHC) and color reflected that the difference between the LVEF-treated (1.20 kV/m) group and the fresh groups was the smallest. The oxidation analysis of protein showed that the LVEF-treated group had smaller values of carbonyl concentration ($0.0551 \pm 0.0048\ \mu$mol/g), larger values of sulfhydryl concentration ($0.737 \pm 0.0364\ \mu$mol/g), and higher Ca^{2+}-ATPase activity (30.10 ± 1.52 U/g) than the C4 group ($0.0649 \pm 0.0013\ \mu$mol/g, $0.510 \pm 0.0225\ \mu$mol/g, and 25.18 ± 1.42 U/g, respectively). SDS-PAGE demonstrated the ability of LVEF to inhibit the hydrolysis and cross-linking of proteins. Meanwhile, the LVEF-treated group had lower values of TBARs ($2.26 \pm 0.0371\ \mu$g/kg) than the other groups and had a lower lipid oxidation level. In addition, the fatty acids in the LVEF-treated group were similar to those in the fresh group and were beneficial to human health. In conclusion, LVEF (1.20 kV/m) could inhibit protein and lipid oxidation of PM during chilled storage.

1. Introduction

Pigeon meat (PM) is the fourth crucial poultry meat because of its unique flavor and high value of nutrition [1]. It is worth noting that the problem of imperfect PM preservation technologies is also exposed with the increase in PM yield. Outdated preservation techniques are more likely to contribute to the oxidation of proteins and lipids, which can lead to a decrease in the edible quality of meat. Proteins and lipids are the main components of meat and the dominant contributors to juiciness, tenderness, flavor, and aroma [2]. Proteins in meat have a wide variety of types and functions, but oxidized proteins are all subject to aggregation or degradation, altering the original construction of the protein [3]. For example, oxidation can change the charge distribution of amino acid residues and expose the hydrophobic core of proteins, reducing the number of hydrogen bonds between proteins and water molecules and leading to water loss in meat [4]. In addition, disulfide bonds and carbonyl groups formed as a result of protein oxidation can lead to the cross-linking of proteins, resulting in decreased meat tenderness [5]. Oxidation of lipids should be noticed as well. It has been found that phospholipids on cell membranes can be oxidized, leading to leakage of cell contents, including

reactive oxygen species (ROS), which refers to both free and nonfree radicals of oxygen origin, such as OH^-, O_2^-, and H_2O_2 [6]. This phenomenon exacerbates the oxidation of meat, further contributing to the rupture of the cell membrane [7]. In addition, lipid oxidation may transfer oxidative stress to proteins and affect the PM quality through protein oxidation [8]. Various preservation techniques have been developed and applied to inhibit oxidation, including low-voltage electrostatic field (LVEF), which is a technology that imposes an electric field environment during food processing.

LVEF is widely used to assist in the freezing or thawing of meat and its products, which can inhibit protein oxidation and improve WHC and tenderness, such as pork steaks [9], beef steaks [10], and chicken breast [11]. The preservation mechanism of LVEF is that the electrostatic field enables the directional movement of ions with different charges and increases the heat transfer coefficient, which is beneficial in reducing the damage of ice crystals to muscle cells [12]. Therefore, the movement of charged ions in the presence of LVEF may inhibit the production of ROS in PM and change the charge distribution of biomolecules, reducing the chances of proteins and lipids reacting with ROS to inhibit PM oxidation. Modified atmosphere packaging (MAP) is a preservation technique used to extend the shelf life of meat by changing the type and proportion of filling gas [2]. Oxygen, carbon dioxide, and nitrogen are the most common filling gases. Oxygen not only inhibits the growth of anaerobic microorganisms but also promotes the oxidation of biomolecules. Therefore, adjusting the oxygen-to-carbon dioxide ratio may inhibit this oxidation reaction and extend the shelf life of foods. Electron beam irradiation (EBI) is a preservation technology that utilizes high-energy electron beam processing of food, which is widely used to inactivate microorganisms and extend the shelf life of food [5]. Therefore, this study was able to better demonstrate the inhibitory effects of different nonthermal preservation techniques on protein and lipid oxidation by using LVEF, MAP, or EBI to preserve PM. This work can provide data to support the promotion of nonthermal preservation techniques.

This study aimed to determine the inhibitory effects of LVEF, MAP, and EBI on PM protein and lipid oxidation under chilling storage to identify an appropriate strategy for PM preservation. Meanwhile, PCA and PLS-DA were used to evaluate the effects of three preservation techniques on the main fatty acid composition of PM. Based on the perspective of inhibiting protein and lipid oxidation, this paper aimed to find a suitable preservation method that could be used to improve the water-holding capacity, color, and texture of PM and to extend the shelf life of PM.

2. Materials and Methods

2.1. Sample and Material Preparation. The pigeons were purchased from Shanghai Shen Yu Pigeon Breeding Professional Cooperative for European Pigeons (Shanghai, China), approximately 1 month old (161.0 ± 11.6 g). The pigeon was slaughtered, cleaned, and had its viscera removed. After removing the head and neck, the pigeons were transported to the laboratory within 2 hours under an ice bath. Next, the pigeons were halved along the spine, cleaned, wiped dry, and packed using a MAP-H360 Compound Gas Preservation Packaging Machine (Suzhou Senrui Preservation Equipment Co., Ltd., Jiangsu, China). The sample number for each time point (0, 5, 10, 15, and 20 days) for each treatment group (C4, MA, MB, MC, EA, EB, EC, and LV) was 5. As shown in Figure 1, each treatment group consisted of C4 (refrigerated storage only; the actual temperature was 3 ± 1°C), MA (50% CO_2 + 50% N_2), MB (10% O_2 + 40% CO_2 + 50% N_2), MC (20% O_2 + 30% CO_2 + 50% N_2), EA (2 kGy), EB (4 kGy), EC (8 kGy), and LV (1.20 kV/m). The treated samples were placed together in a cold store (3 ± 1°C), and the temperature changes in the cold store were monitored in real time. Test samples were taken from the pigeon breast meat, and the obtained meat samples were frozen at −80°C for the following testing.

N_2, CO_2, and O_2 were obtained from Shanghai Jiajie Specialty Gases Co., Ltd. (Shanghai, China). EBI was provided by Shanghai Suneng Fuzhao Technology Co., Ltd. (Shanghai, China). DENBA Japan Co., Ltd., provided the LVEF device (model). The Protein Carbonyl Assay Kit, the Total Mercapto Assay Kit, and the Tris-Tricine-SDS-PAGE Gel Preparation Kit were purchased from Beijing Solarbio Science & Technology Co., Ltd. (Beijing, China). The CheKine™ Ca^{2+}/Mg^{2+}-ATPase Activity Assay Kit was purchased from Abbkine Scientific Co., Ltd. (Hubei, China). 3-Color Prestained Protein Standards (AG11919) were purchased from Accurate Biotechnology Co., Ltd. (Hunan, China). The Chicken Thiobarbituric Acid Reactor ELISA Kit was purchased from Jiangsu Meimian Industrial Co., Ltd. (Jiangsu, China). Methyl alcohol and heptane are used for HPLC reagents. The other reagents are analytical reagents. All the reagents were purchased from Sinopharm Chemical Reagent Co., Ltd. (Shanghai, China). Supelco 37 Component FAME Mix was purchased from Shanghai Yuanye Bio-Technology Co., Ltd. (Shanghai, China).

2.2. Physicochemical Parameters

2.2.1. Color. The color measurement was performed as described by Wyrwisz et al. [13], with slight modifications. Each group has 5 parallel samples, and each sample was tested three times. The PM was measured by CM-5 colorimeter (Hangzhou Ke Sheng Instrument Co., Ltd.) with the following parameters: 8 mm measuring aperture, SCE, light source D65, 10° standard observer, and white plate correction ($L^* = 96.45$, $a^* = -0.14$, and $b^* = -0.28$).

2.2.2. Storage Loss, Cooking Loss, and Centrifuging Loss. Storage loss was calculated from the mass of the PM before storage (recorded the mass as m_0) and after storage (m_1) with the following equation:

$$\text{Storage loss}\,(\%) = \frac{m_0 - m_1}{m_0} \times 100\%. \quad (1)$$

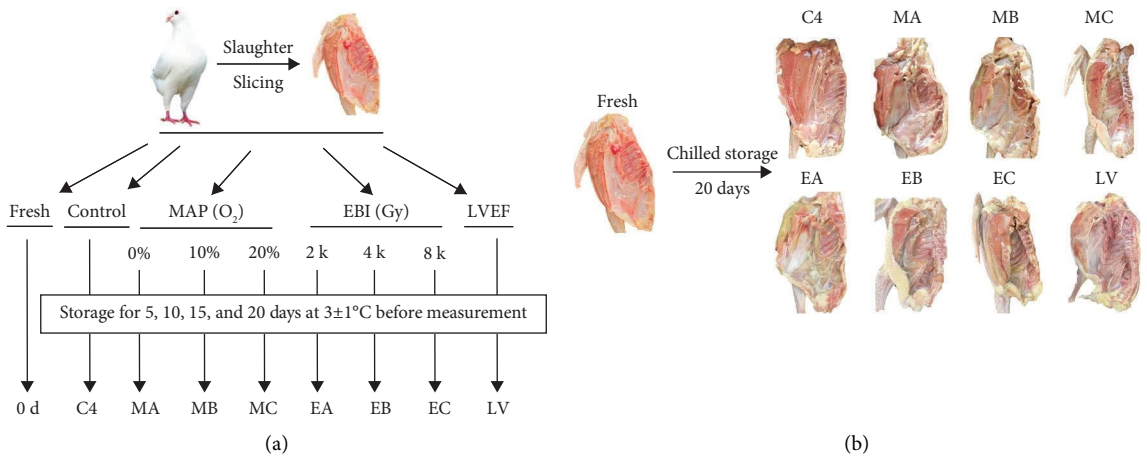

Figure 1: Schematic diagram showing the experimental design (a) and picture of PM from each group on the 20th day (b). C4 (refrigerated storage only), MA (50% CO_2 + 50% N_2), MB (10% O_2 + 40% CO_2 + 50% N_2), MC (20% O_2 + 30% CO_2 + 50% N_2), EA (2 kGy), EB (4 kGy), EC (8 kGy), and LV (1.20 kV/m).

Cooking loss was determined with slight modifications according to the method of Li et al. [14]. PM (record the mass as m_2) was placed in polyethylene bags and vacuum sealed. Next, the PM was boiled in 85°C water until the central temperature reached 72°C. A needle temperature sensor was pierced through a polyethylene bag into the PM to measure the center temperature of the meat in real time. It was then cooled to room temperature under running water and swabbed dry to record the mass as m_3, calculated as follows:

$$\text{Cooking loss}\,(\%) = \frac{m_2 - m_3}{m_2} \times 100\%. \quad (2)$$

The centrifuging loss was determined according to the method of Wang et al. [15] with slight modifications. 1 g of PM (recorded the mass as m_4) was weighed in a 10 ml centrifuge tube and centrifuged at 20°C, 10,000 g, for 10 min. The centrifuged PM was wiped dry and weighed as m_5, calculated as follows:

$$\text{Centrifuging loss}\,(\%) = \frac{m_4 - m_5}{m_4} \times 100\%. \quad (3)$$

2.2.3. Texture Analysis. PM after the determination of cooking loss was used to determine shear force [14]. Each PM sample was trimmed into a rectangular shape (5 cm * 5 cm * 2 cm, length, width, and height), and the muscle fibers were placed perpendicular to the direction of shear force. The parameters of the texture analyzer (TA-XT Plus, Stable Micro System, LOTUN SCIENCE Co., Ltd., China) configured with A/MORS were as follows: pretest speed and test speed were 1.5 mm/s, posttest speed was 10 mm/s, depth was 8 mm, and trigger force was 20 g.

2.3. Determination of Carbonyl Concentration. The carbonyl concentration of PM was determined using the Protein Carbonyl Assay Kit (Beijing Solarbio Science & Technology Co., Ltd., China; cat#BC1275). 0.1 g (accurate to 0.0001 g) of pigeon breast meat was weighed, and 1 mL of extraction buffer was added and homogenized in an ice bath for 1 min. The sample was centrifuged at 5000 rpm for 10 min at 4°C. The supernatant was used for the assay. The test solution was prepared according to the instructions. Finally, the absorbance of the test solution was measured at 370 nm, and the carbonyl concentration was calculated.

2.4. Determination of Sulfhydryl (SH) Concentration. The sulfhydryl concentration of PM was determined using the Total Mercapto Assay Kit (Beijing Solarbio Science & Technology Co., Ltd.; cat#BC1375). 0.1 g (accurate to 0.0001 g) of pigeon breast meat was weighed, and 1 mL of extraction buffer was added and homogenized in an ice bath for 1 min. The sample was centrifuged at 8000 g for 10 min at 20°C. The supernatant was used for the assay. The test solution was prepared according to the instructions. The standard curve was plotted according to the standard (glutathione) provided in the kit and the instructions, and $R^2 > 0.99$ was required. Finally, the absorbance of the test solution was measured at 412 nm, and the sulfhydryl concentration was calculated based on the standard curve.

2.5. Determination of Ca^{2+}-ATPase Activity. The CheKine™ Ca^{2+}/Mg^{2+}-ATPase Activity Assay Kit (Abbkine Scientific Co., Ltd., China; cat#KTB1810) was used to measure the Ca^{2+}-ATPase activity of PM. 0.1 g (accurate to 0.0001 g) of pigeon breast meat was weighed, and 1 mL of extraction buffer was added and homogenized in an ice bath for 1 min. The sample was centrifuged at 8000 g for 10 min at 4°C. The supernatant was used for the assay. The test solution was prepared according to the instructions. Finally, the absorbance of the test solution was measured at 660 nm, and the Ca^{2+}-ATPase activity was calculated.

2.6. Sodium Dodecyl Sulfate-Polyacrylamide Gel Electrophoresis (SDS-PAGE). Myofibrillar proteins (MPs) were prepared according to Hirasaka et al. [16], with some

modifications. 0.02 g of PM was weighed into 200 μL protein extraction solution and homogenized on ice for 3 min. Then, the sample was centrifuged at 12000 rpm for 20 min at 4°C to obtain the supernatant. The protein concentration was determined by the biuret method [17]. Then, protein profiles of MPs of PM were analyzed by SDS-PAGE, based on the method described by Liu et al. [18]. SDS-PAGE with 5% stacking gel and 12% separating gel was used. The protein (1 mg/mL), mixed with the sample loading buffer (with or without 1 M β-mercaptoethanol (ME)) at the ratio of 4 : 1 (v/v), was heated in boiling water for 5 min. An aliquot of 10 μL of samples was loaded onto the gel. Then, the gel was subjected to electrophoresis at a voltage of 80 V for 25 min and 120 V for 45 min. The gel was immersed in a stained solution (0.25 g/L Coomassie Brilliant Blue R-250 dissolved in 25% ethanol (v/v) and 8% acetic acid (v/v)) for 5 h and then immersed in a destained solution (25% ethanol (v/v) and 8% acetic acid (v/v)) for 3 h.

2.7. Thiobarbituric Acid-Reactive Substance (TBAR) Assay. The Chicken Thiobarbituric Acid Reactor ELISA Kit (Jiangsu Meimian Industrial Co., Ltd., Jiangsu, China) was used to determine the concentration of TBARs in PM. According to the instructions of the kit, the sample to be tested and the detection antibody HRP were added to the microtiter wells of the enzyme plate coated with TBAR antibody, prewarmed (37°C, 60 min), and washed thoroughly. The absorbance (OD) was measured at 450 nm using the substrate TMB as the chromogenic reagent, and the concentration of TBARs in the test sample was calculated from the linear regression curve of the standard. The standard curve was plotted according to the standard provided in the kit and the instructions, and $R^2 > 0.99$ was required.

2.8. Determination of Fatty Acid. The fatty acid contents of the PM sample were analyzed following the method described by Jo et al. [19]. In brief, 2 g of minced PM was mixed with 100 mg of pyrogallol, 2 mL of internal standard solution (1,2,3-triundecanoyl glycerol, for GC), 2 mL of 95% ethanol, and 10 mL of 8.3 M HCl and hydrolyzed for 40 min at 80°C. The hydrolyzed sample was extracted three times with a mixture of ether and petroleum ether in equal proportion. Next, the extract was evaporated to dryness, and sodium hydroxide and methanol were added to generate the fatty acid methyl ester. Then, heptane (for HPLC) was added to extract the fatty acid methyl ester, and anhydrous sodium sulfate was used to remove water. Finally, the supernatant was obtained after centrifugation.

The supernatant was detected by gas chromatography-mass spectrometry (GC-MS) equipped with a flame ionization detector (GC:TRACE 1300; MS: ISQ 7000; Thermo Fisher Scientific, Waltham, Massachusetts, USA) and capillary GC column (DB-5MS, 30 m × 0.25 mm × 0.25 μm) (Agilent Technologies, Palo Alto, USA). The injection volume of the sample was 1 μL, and helium was used as the gas carrier. The injector temperature was 270°C. The split flow was 5 mL/min, and the split ratio was 5. The constant flow was 1 mL/min. The GC heating program was as follows: 90°C for 1 min; 8°C/min up to 170°C; 5°C/min up to 240°C; and, finally, 25°C/min up to 290°C and held for 7 min. The mass spectra were recorded in electron impact (EI) ionization mode at 70 eV. The ion source temperature was 250°C, the transfer line temperature was 280°C, and the scans were carried out at intervals of 0.2 s in the range of 33~550 amu ion mass-to-charge ratios (m/z).

2.9. Statistical Analysis. The number of experimental samples in parallel was 5. The results were taken as the mean of 5 data. Different statistical methods such as one-way ANOVA, Duncan's test, principal component analysis (PCA), and partial least-squares regression discriminant analysis (PLS-DA) were applied to the data set. One-way ANOVA and Duncan's test were conducted using SPSS version 20. The histograms were constructed using Origin version 2018. PCA and PLS-DA were conducted using MetaboAnalyst 5.0.

3. Results and Discussion

3.1. Physicochemical Parameters

3.1.1. Color. The changes in color under nonthermal technologies were evaluated using L^*, a^*, and b^* values. As shown in Table 1, a^* value (redness value) showed a gradually rising trend among all groups due to the oxidation of myoglobin (Mb). The proportion of three forms of Mb was a key factor affecting PM color [20]. Brown methemoglobin (MMb) was the final oxidation product of Mb, which could considerably decrease the red color of PM. On the 20th day, the a^* values tended to decrease in all groups, with the LV group having the highest a^* values, which was related to the increase in the relative proportion of high iron myoglobin in PM. There was no significant difference in the b^* value between all groups ($p > 0.05$), but it was higher than that of the fresh group (0 d). Research has shown that the b^* value was positively correlated with the level of lipid oxidation [21]. The b^* value change in PM indicated that all groups were oxidized during chilled storage. The L^* value continuously increased with the extension of storage time. The exudate of the PM could form a water film on the surface of the meat, which increases the L^* value [22]. It was worth noting that the three nonthermal technologies did not significantly impact the L^* value ($p > 0.05$).

3.1.2. WHC. Water loss could affect the weight, appearance, and sensory properties of meat products [23]. The effect of nonthermal technologies on the WHC of PM is shown in Figure 2. With the extension of storage time, the storage loss increased in all groups (Figure 2(a)), which revealed that the WHC of PM was decreasing. It was noteworthy that the storage loss of the LV group (6.89 ± 0.38%) was significantly higher than that of the other groups ($p < 0.05$). This phenomenon was due to changes in the static charge of muscle filaments in the electrostatic field, reducing the distance between muscle filaments [4]. The centrifuging loss showed an increasing trend (Figure 2(b)), which indicated

Table 1: Effect of nonthermal technologies on the color of PM.

Color	Group	0 d	5 d	10 d	15 d	20 d
a^* value	C4	15.78 ± 0.73	17.73 ± 1.40^{abc}	16.67 ± 1.940^{abc}	18.30 ± 1.89^{a}	16.55 ± 1.19^{ac}
	MA		17.74 ± 1.40^{abc}	16.19 ± 1.30^{abc}	16.59 ± 1.82^{ac}	15.79 ± 2.50^{ac}
	MB		19.49 ± 1.98^{b}	17.91 ± 1.55^{b}	15.88 ± 1.34^{ac}	12.10 ± 1.84^{b}
	MC		16.83 ± 1.37^{abc}	17.00 ± 1.45^{ab}	22.53 ± 1.72^{b}	15.85 ± 0.57^{ac}
	EA		15.33 ± 1.99^{c}	15.53 ± 0.97^{ac}	16.62 ± 1.04^{ac}	16.40 ± 1.57^{ac}
	EB		18.72 ± 1.79^{ab}	15.29 ± 0.52^{ac}	16.18 ± 1.35^{ac}	14.93 ± 1.47^{c}
	EC		15.56 ± 0.92^{c}	15.31 ± 0.42^{ac}	15.39 ± 0.73^{c}	14.54 ± 1.12^{c}
	LV		16.52 ± 1.70^{abc}	14.49 ± 0.39^{c}	17.22 ± 1.07^{ac}	17.16 ± 1.22^{a}
b^* value	C4	14.03 ± 1.95	17.24 ± 2.48^{a}	16.64 ± 2.01^{a}	18.78 ± 2.21^{a}	17.29 ± 2.19^{a}
	MA		17.40 ± 2.67^{a}	16.86 ± 0.92^{a}	18.55 ± 1.03^{a}	17.23 ± 2.08^{a}
	MB		17.05 ± 2.12^{a}	18.65 ± 0.84^{b}	17.05 ± 2.12^{a}	18.23 ± 1.17^{a}
	MC		17.04 ± 1.82^{a}	16.12 ± 0.70^{a}	19.64 ± 1.11^{a}	18.22 ± 0.51^{a}
	EA		15.75 ± 2.28^{a}	16.97 ± 0.42^{a}	18.36 ± 1.71^{a}	19.35 ± 2.37^{a}
	EB		16.24 ± 2.59^{a}	16.21 ± 1.03^{a}	17.74 ± 2.05^{a}	17.22 ± 1.21^{a}
	EC		16.41 ± 0.81^{a}	16.57 ± 1.10^{a}	17.57 ± 2.18^{a}	17.03 ± 0.74^{a}
	LV		15.98 ± 1.89^{a}	15.43 ± 1.86^{a}	17.61 ± 2.16^{a}	17.88 ± 1.38^{a}
L^* value	C4	36.25 ± 3.09	41.97 ± 1.22^{a}	40.59 ± 1.82^{a}	41.63 ± 1.04^{a}	42.16 ± 1.52^{ab}
	MA		41.15 ± 1.23^{a}	41.28 ± 2.16^{a}	42.56 ± 1.30^{a}	42.89 ± 2.86^{abc}
	MB		40.54 ± 1.43^{a}	41.31 ± 2.61^{a}	41.90 ± 2.14^{a}	45.73 ± 1.49^{c}
	MC		40.92 ± 2.86^{a}	39.32 ± 1.70^{a}	40.20 ± 1.35^{a}	43.20 ± 1.28^{abc}
	EA		39.43 ± 3.06^{a}	42.12 ± 1.77^{a}	42.89 ± 2.01^{a}	44.52 ± 0.61^{bc}
	EB		38.72 ± 3.75^{a}	40.23 ± 2.25^{a}	41.81 ± 1.25^{a}	42.35 ± 2.24^{ab}
	EC		41.30 ± 1.55^{a}	41.30 ± 1.85^{a}	42.97 ± 3.14^{a}	43.17 ± 2.22^{abc}
	LV		38.72 ± 1.94^{a}	40.73 ± 3.09^{a}	40.16 ± 3.44^{a}	41.33 ± 3.13^{a}

Note. Different lowercase letters (a to c) indicate that there are significant differences among the treatment groups on the same day ($p < 0.05$). C4 (refrigerated storage only), MA (50% CO_2 + 50% N_2), MB (10% O_2 + 40% CO_2 + 50% N_2), MC (20% O_2 + 30% CO_2 + 50% N_2), EA (2 kGy), EB (4 kGy), EC (8 kGy), and LV (1.20 kV/m).

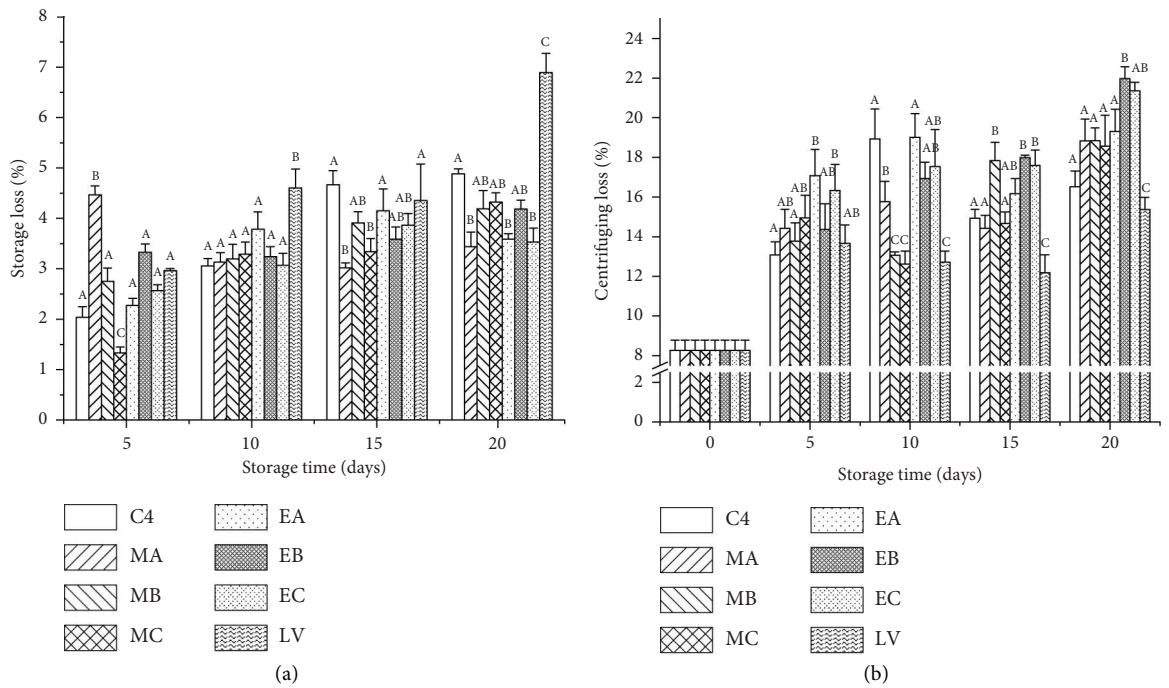

Figure 2: Continued.

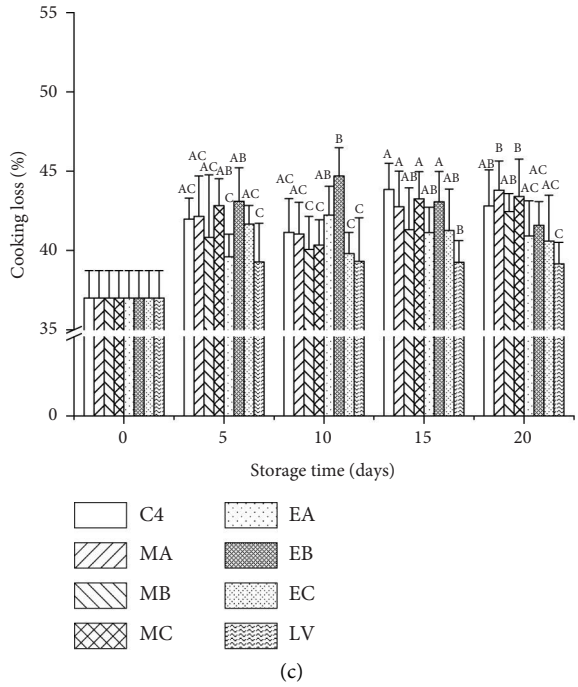

Figure 2: Effect of nonthermal technologies on the WHC of PM. Different uppercase letters (A to C) indicate that there are significant differences among the treatment groups on the same day ($p < 0.05$). C4 (refrigerated storage only), MA (50% CO_2 + 50% N_2), MB (10% O_2 + 40% CO_2 + 50% N_2), MC (20% O_2 + 30% CO_2 + 50% N_2), EA (2 kGy), EB (4 kGy), EC (8 kGy), and LV (1.20 kV/m).

a weakening of the interaction force between muscle and water, and the oxidative denaturation of proteins was closely related to this process. The results showed that the centrifuging loss was generally higher in the EBI-treated groups (EA group was 19.31 ± 1.12%, EB group was 21.97 ± 0.60%, and EC group was 21.36 ± 0.42%) than that of the other groups ($p < 0.05$). Because the ROS produced by irradiation led to the oxidation of protein [24], protein oxidation exposed its internal hydrophobic core, weakening the interaction force between protein and water molecules and increasing the centrifugal loss rate. In addition, the lowest centrifuging loss was observed in the LV group (15.36 ± 0.62%) because LVEF could cause resonance phenomena of water molecules and proteins within the muscle, reducing the loss of water from the muscle. The results of the cooking loss rate of PM are shown in Figure 2. The lowest cooking loss (39.15 ± 1.35%) was observed in the LV group on the 20th d, which indicates that the low-voltage electrostatic field is more effective in stabilizing the equilibrium of protein intermolecular and protein-water molecule interactions.

3.1.3. Tenderness. The tenderness of meat had a major impact on consumer satisfaction and was usually determined by the shear force value. As shown in Table 2, an increasing trend of tenderness was found in all groups during chilled storage, which might be due to cellular autolysis or protein breakdown by spoilage microorganisms. On the 5th day, the MC and EC groups showed a significantly lower shear force than the C4 group ($p < 0.05$), which indicated that the tenderness of PM (MC and EC groups) increased. It was noteworthy that the shear force of the EA group was significantly higher than that of the other groups ($p < 0.05$). This phenomenon was due to the lower irradiation dose of the EA group, which caused ROS generated in the cells, leading to the cross-linking of proteins and reducing the tenderness of the PM [5]. As the irradiation dose increased (e.g., in the EB and EC groups), the concentration of ROS in the cells increased. In this case, protein cross-linking also occurred, and autolysis occurred in many muscle cells, which reduced the tightness of the muscle and made the PM more tender [25]. Until the 20th day, the shear force of the samples (LV group) was lower than that of the other groups ($p < 0.05$), implying that LVEF was able to induce an increase in the tenderness of PM. In contrast, the shear force of the EA and EB groups was higher than that of the other groups, which was the result of the constant oxidation of proteins by ROS generated by irradiation.

3.2. Protein Oxidation

3.2.1. Carbonyl Concentration of PM. The carbonyl group was the most widely used indicator of protein oxidation and was one of the main factors contributing to the deterioration of meat quality [26]. Figure 3(a) demonstrates the effect of nonthermal technologies on the carbonyl concentration of PM. The result showed that the carbonyl concentration of PM increased with time, and the carbonyl concentration was 0.0441 μmol/g on 0 d. During the first 5 d, the carbonyl concentrations of the EB and EC groups increased, which were significantly higher than those of the other groups ($p < 0.05$). The maximum carbonyl concentration of each group (C4, MA, MB, MC, EA, EB, EC, and LV) reached

Table 2: Effect of nonthermal technologies on the shear force of PM.

Group	0 d (*N*)	5 d (*N*)	10 d (*N*)	15 d (*N*)	20 d (*N*)
C4	11.77 ± 0.73	11.89 ± 0.64^{a}	11.75 ± 1.28^{abd}	9.93 ± 0.83^{a}	10.63 ± 0.73^{a}
MA		11.90 ± 0.99^{a}	11.09 ± 0.80^{abc}	10.74 ± 0.31^{b}	10.46 ± 1.01^{a}
MB		12.25 ± 1.01^{a}	10.15 ± 0.88^{c}	10.41 ± 0.66^{ab}	11.38 ± 0.90^{b}
MC		10.78 ± 0.98^{b}	12.68 ± 1.08^{d}	11.42 ± 0.80^{c}	11.42 ± 0.97^{b}
EA		13.80 ± 1.03^{c}	12.01 ± 1.18^{ad}	11.44 ± 0.72^{c}	12.16 ± 1.08^{cd}
EB		12.01 ± 0.71^{a}	11.05 ± 1.10^{abc}	11.20 ± 1.53^{c}	12.68 ± 0.74^{d}
EC		10.85 ± 0.66^{b}	12.85 ± 1.20^{d}	11.39 ± 0.83^{c}	11.77 ± 0.88^{bc}
LV		11.52 ± 0.83^{ab}	10.46 ± 0.85^{bc}	10.27 ± 0.94^{ab}	10.14 ± 1.06^{a}

Note. Different lowercase letters (a to d) indicate that there are significant differences among the treatment groups on the same day ($p < 0.05$). C4 (refrigerated storage only), MA (50% CO_2 + 50% N_2), MB (10% O_2 + 40% CO_2 + 50% N_2), MC (20% O_2 + 30% CO_2 + 50% N_2), EA (2 kGy), EB (4 kGy), EC (8 kGy), and LV (1.20 kV/m).

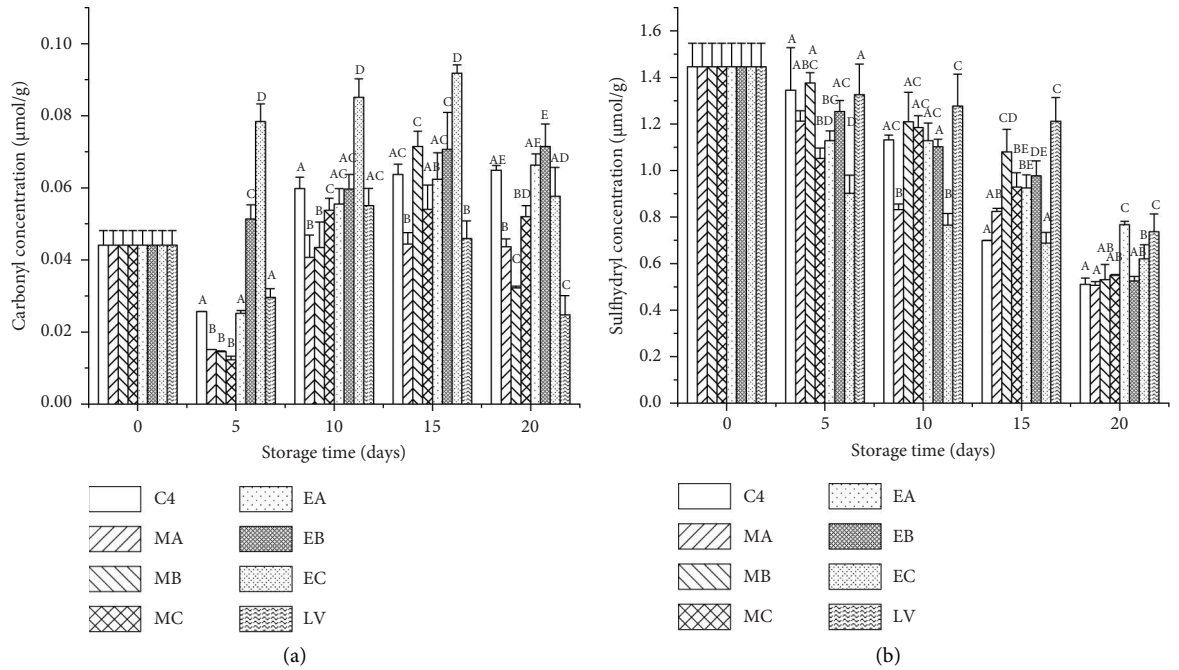

Figure 3: Continued.

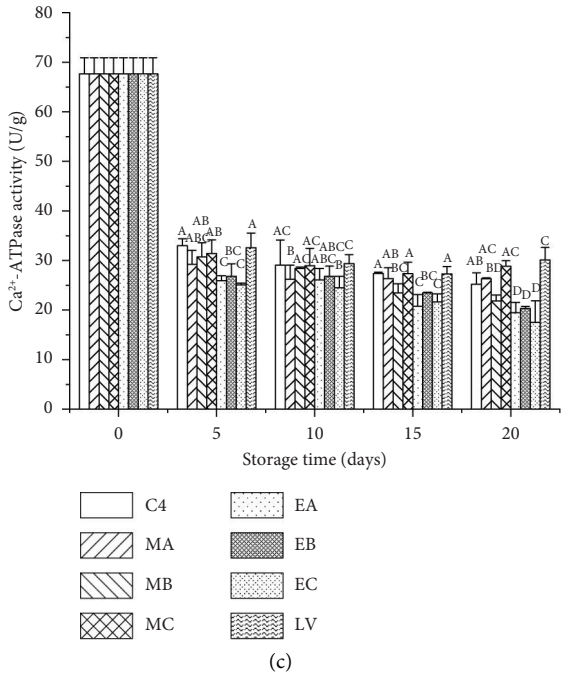

Figure 3: Changes in the (a) carbonyl and (b) sulfhydryl group concentrations of PM and (c) Ca^{2+}-ATPase activity of PM during chilled storage. Different uppercase letters (A to E) indicate that there are significant differences among the treatment groups on the same day ($p < 0.05$). C4 (refrigerated storage only), MA (50% CO_2 + 50% N_2), MB (10% O_2 + 40% CO_2 + 50% N_2), MC (20% O_2 + 30% CO_2 + 50% N_2), EA (2 kGy), EB (4 kGy), EC (8 kGy), and LV (1.20 kV/m).

0.0649 μmol/g, 0.0444 μmol/g, 0.0715 μmol/g, 0.0541 μmol/g, 0.0664 μmol/g, 0.0715 μmol/g, 0.0918 μmol/g, and 0.0551 μmol/g during chilled storage, respectively. The lowest carbonyl concentrations were found in groups MA, MC, and LV. The carbonyl concentration of samples treated with MAP or LVEF was consistently lower than that of the C4 group. This phenomenon indicated that MAP and LVEF could effectively inhibit protein oxidation. The carbonyl concentration of the EBI-treated groups was significantly higher than that of the other groups before 15 d ($p < 0.05$). This phenomenon meant that EBI could accelerate the oxidation of proteins. In addition, on the 20th day, the carbonyl concentrations of the MB and LV groups were significantly lower than those of the other groups ($p < 0.05$). Meanwhile, the carbonyl concentrations of the MB, EC, and LV groups decreased rapidly from 15 d to 20 d ($p < 0.05$). The main reason for the change in carbonyl concentration might be the increase in the exudate loss.

The main cause of carbonyl formation was ROS, which attack amino acid side chains and polypeptide backbones [27]. The carbonyl concentration of the EBI-treated groups was higher than that of the other groups. This was attributed to the fact that EBI produced more ROS than other groups. EBI interacts with water molecules, causing the dissociation of water molecules to produce hydroxyl radicals (·OH), while hydroxyl radicals interact with oxygen molecules to produce more ROS than in the C4 group [5]. The carbonyl concentrations were lower in the MAP-treated groups (MA, MB, and MC groups) than that in the C4 group. This was attributed to the fact that CO_2 in MAP could be an acceptor of electrons, inhibiting electron transfer and producing fewer ROS than in the C4 group [28]. However, LVEF could alter the charge distribution of biomolecules, inhibit cellular metabolism, and reduce ROS production [29]. The formation of carbonyl functional groups was usually accompanied by cross-linking and fragmentation of the protein [30]. Although the carbonyl concentration was less than 2 μmol/g in all groups, cross-linking still occurred and affected the color, water-holding capacity, and tenderness of PM [2].

3.2.2. Sulfhydryl Concentration of PM. Sulfhydryl functional groups were one of the most active functional groups in proteins [31]. As shown in Figure 3(b), sulfhydryl concentration decreased during chilled storage, and the fresh group was 1.45 μmol/g. On the 5th day, the sulfhydryl concentrations of the EC groups were significantly lower than those of the other groups ($p < 0.05$) because the higher ROS concentration significantly increases the oxidation rate of sulfhydryl groups. The LV group had a higher sulfhydryl concentration in all groups and showed significant differences at 10 d and 15 d ($p < 0.05$). On the 20th day, the highest sulfhydryl concentration was found in the EA and LV groups ($p < 0.05$). It was indicated that LVEF could effectively inhibit the oxidation of the sulfhydryl functional groups. The C4 group showed the greatest decrease in sulfhydryl concentration from 10 d to 15 d, while the other groups occurred from 15 d to 20 d. This phenomenon might be because the C4 group could accumulate ROS faster. Notably, there was no significant difference between the groups (C4, MA, MB, and MC) on the 20th day. This phenomenon might be due to the number of sulfhydryl

functional groups that could participate in the reaction having reached a threshold.

During chilled storage, the sulfhydryl groups of cysteine were oxidized by ROS to disulfide bonds (-S-S-), resulting in a decrease in sulfhydryl concentration [32]. Disulfide bonding was one of the common ways of protein cross-linking and a key marker of sulfhydryl oxidation [6]. Cross-linking of proteins could alter the conformation and function of MPs, which, in turn, affects the quality of PM. Therefore, a higher sulfhydryl concentration could maintain the better quality of PM.

3.2.3. Ca^{2+}-ATPase Activity of PM. Ca^{2+}-ATPase activity could reflect the integrity and superior quality of MPs [33]. As shown in Figure 3(c), the Ca^{2+}-ATPase activity of PM showed a significant decrease during chilled storage ($p < 0.05$). This phenomenon indicated that the quality of MPs decreases continuously with storage time, especially in the first 5 days. This phenomenon was associated with conformational changes in myosin globular heads, increased protein-protein interactions, and ionic strength [34]. The Ca^{2+}-ATPase activity of the fresh group was 67.66 ± 3.25 U/g. The sink rate of each group (C4, MA, MB, MC, EA, EB, EC, and LV) about the Ca^{2+}-ATPase activity was 51.27%, 56.82%, 54.61%, 53.62%, 61.66%, 60.39%, 62.93%, and 51.84%, respectively. The EBI-treated groups showed the fastest decline during the first 5th day ($p < 0.05$), which was mainly due to the ability of irradiation to produce ROS faster and change the conformation of proteins. From the 5th day, the Ca^{2+}-ATPase activity showed a slow decline in each group. On the 20th day, the enzyme activity of the LV group was significantly higher than that of the other groups ($p < 0.05$), while the enzyme activity of the EBI-treated groups remained the lowest but showed no significant differences between the C4 and MAP-treated groups ($p > 0.05$). The Ca^{2+}-ATPase activity was closely related to the sulfhydryl groups in the globular head of myosin [35]. Oxidation of the sulfhydryl functional groups at the active site of the Ca^{2+}-ATPase would lead to a decline in enzyme activity. The results showed that LVEF could effectively inhibit the oxidation of the sulfhydryl functional groups and the decrease of Ca^{2+}-ATPase activity and could maintain the better structure and function of MPs. It might be that the LVEF changes the charge distribution on the MPs, interfering with the interaction of enzymes or polar molecules with MPs [29].

3.2.4. SDS-PAGE Analysis. The SDS-PAGE results of the MPs are shown in Figure 4. The intensity of the major MP bands contained actin at 43 kDa, troponin T at 38 kDa, tropomyosin at 35 kDa, and troponin T+ at 30 kDa. As the total protein quantity loaded into each lane was constant, the changes in the intensity of protein bands could be attributed to hydrolysis or cross-linking of the protein [10]. In the presence (Figure 4(a)) or absence (Figure 4(b)) of ME, there was no difference in protein intensity between the fresh and LV groups. This phenomenon revealed that LVEF inhibited the cross-linking or degradation of proteins. In the absence of ME, the intensity of actin decreased in the group (C4, MA, MB, MC, EA, EB, and EC). In contrast, in the presence of ME, the intensity of the bands recovered in each group, indicating that cross-linking of actin occurred during chilled storage. The same phenomenon was observed in troponin T in the EBI-treated groups, which might be due to the cross-linking of troponin T in the EBI-treated groups being disulfide bonds. However, the protein intensity of troponin T in the MAP-treated groups was still different compared with the fresh groups. This phenomenon was attributed to Schiff base adducts or the formation of carbon-carbon covalent bonds [36]. Similarly, the results of the tropomyosin and troponin T+ bands showed that cross-linking of proteins with non-disulfide bonds occurred during chilled storage. In the presence of ME, some bands (25–100 kDa) had improved intensity, indicating that disulfide bonds were partially responsible for protein cross-links.

3.3. Lipid Oxidation

3.3.1. TBARs Analysis. TBARs were an indicator of secondary oxidation products such as malondialdehyde (MDA) and were formed during lipid oxidation, and they are commonly used to assess the oxidative rancidity of lipids [37]. The results in Figure 5 showed that lipid oxidation of PM deepened with storage time. On the 5th day, the TBAR value of the C4 group increased rapidly from 2.17 μg/kg to 2.68 μg/kg, significantly higher than that of the other groups ($p < 0.05$), whereas the lowest TBAR values were found in the EC and LV groups ($p < 0.05$). After that, the TBAR values of each group (C4, MA, MB, MB, EA, EB, EC, and LV) showed different levels of increase and reached 3.06 μg/kg, 3.18 μg/kg, 3.03 μg/kg, 2.85 μg/kg, 3.09 μg/kg, 2.41 μg/kg, 3.10 μg/kg, and 2.25 μg/kg. Throughout the storage process, the TBAR value of the LV group was significantly lower in all groups ($p < 0.05$). This phenomenon indicated that LVEF was better able to inhibit lipid oxidation. A decrease in TBAR values was found on the 20th day because lipid oxidation could disrupt the biofilm structure of cells and release ROS into the tissue fluid, which was eventually lost with the exudate. It has also been reported that the ROS were released into the tissue fluid and reacted with more proteins and lipids, accelerating protein and lipid oxidation [6]. The LV group had the lowest values of TBARs, which was consistent with its lower carbonyl concentration. It has been reported that electric fields could alter the charge distribution of tubulin in eukaryotic cells, causing an induced dipole moment and disrupting its function in eukaryotic mitosis [29]. Therefore, the lower TBAR values in the LV group than in the other treatment groups throughout the storage period might also be related to the fact that LVEF decreased the activity of enzymes (e.g., lipoxygenase) associated with lipid oxidation.

3.3.2. Fatty Acid Analysis. The lipid and fatty acid content of meat was a key determinant of its quality characteristics, such as color, texture, and flavor. It has been found that animal species, preservation methods, and cooking methods could influence the lipid and fatty acid content of meat [38].

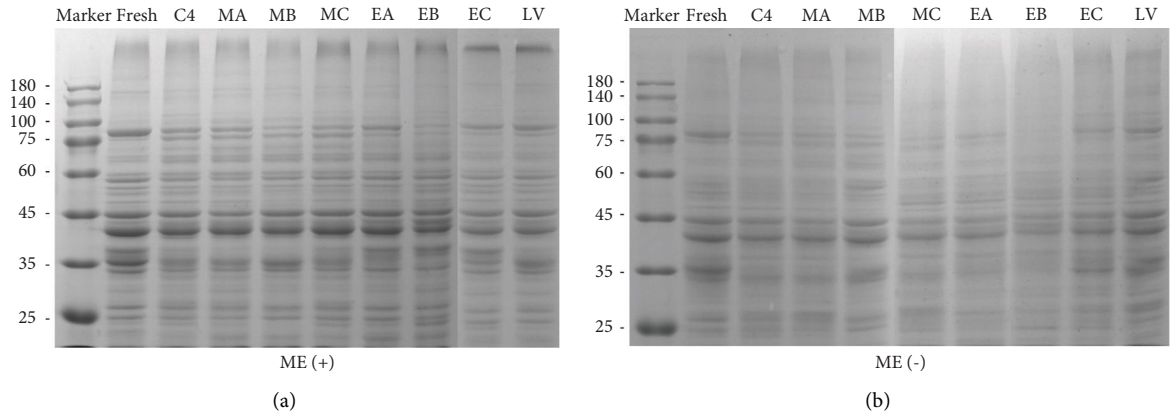

Figure 4: Representative SDS-PAGE patterns of PM during chilled storage. Samples were prepared in the (a) presence and (b) absence of 20% (v/v) 1 M ME. C4 (refrigerated storage only), MA (50% CO_2 + 50% N_2), MB (10% O_2 + 40% CO_2 + 50% N_2), MC (20% O_2 + 30% CO_2 + 50% N_2), EA (2 kGy), EB (4 kGy), EC (8 kGy), and LV (1.20 kV/m).

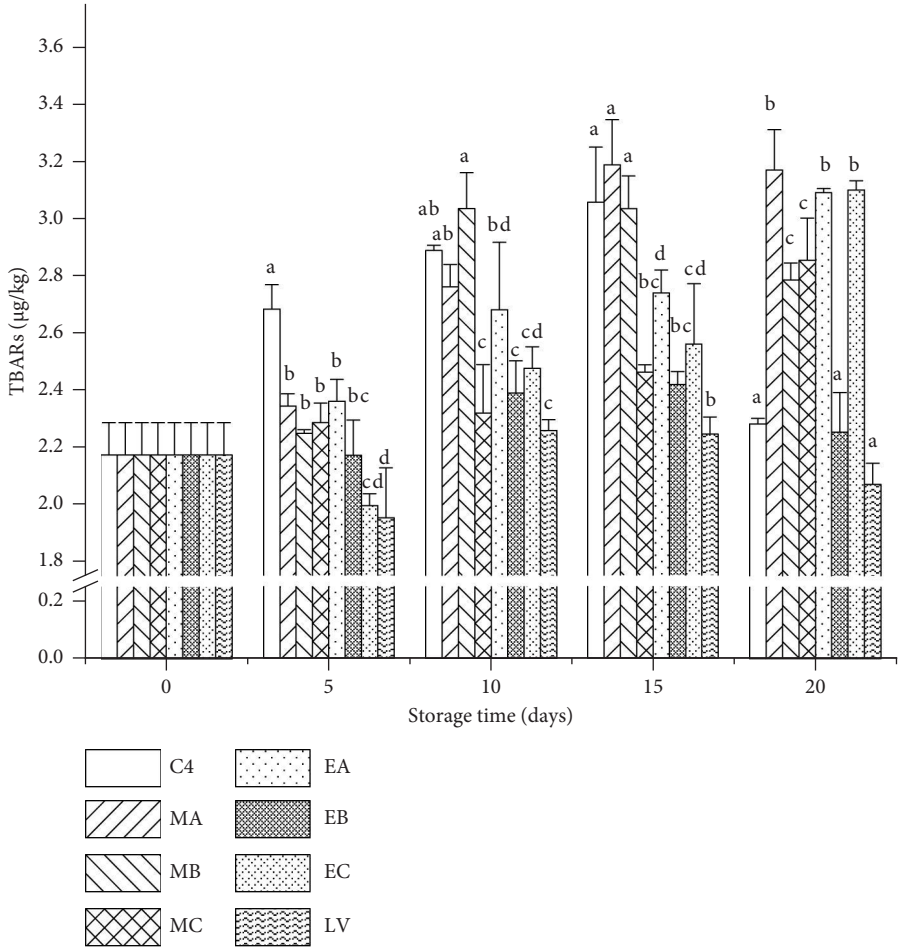

Figure 5: Changes in lipid oxidation of PM. Different lowercase letters (a to d) indicate that there are significant differences among the treatment groups on the same day ($p < 0.05$). C4 (refrigerated storage only), MA (50% CO_2 + 50% N_2), MB (10% O_2 + 40% CO_2 + 50% N_2), MC (20% O_2 + 30% CO_2 + 50% N_2), EA (2 kGy), EB (4 kGy), EC (8 kGy), and LV (1.20 kV/m).

The PCA diagram of the fatty acid composition in the sample is shown in Figure 6(a), with the differences between PC1 and PC2 being 59.1% and 23%, respectively. The results showed that the differences between the C4, MA, EA, EB, EC, LV, and fresh (0 d) groups were the most minor, indicating that the preservation conditions represented by each treatment group could effectively inhibit the hydrolysis or oxidation of fatty acids. Similar situations also occur

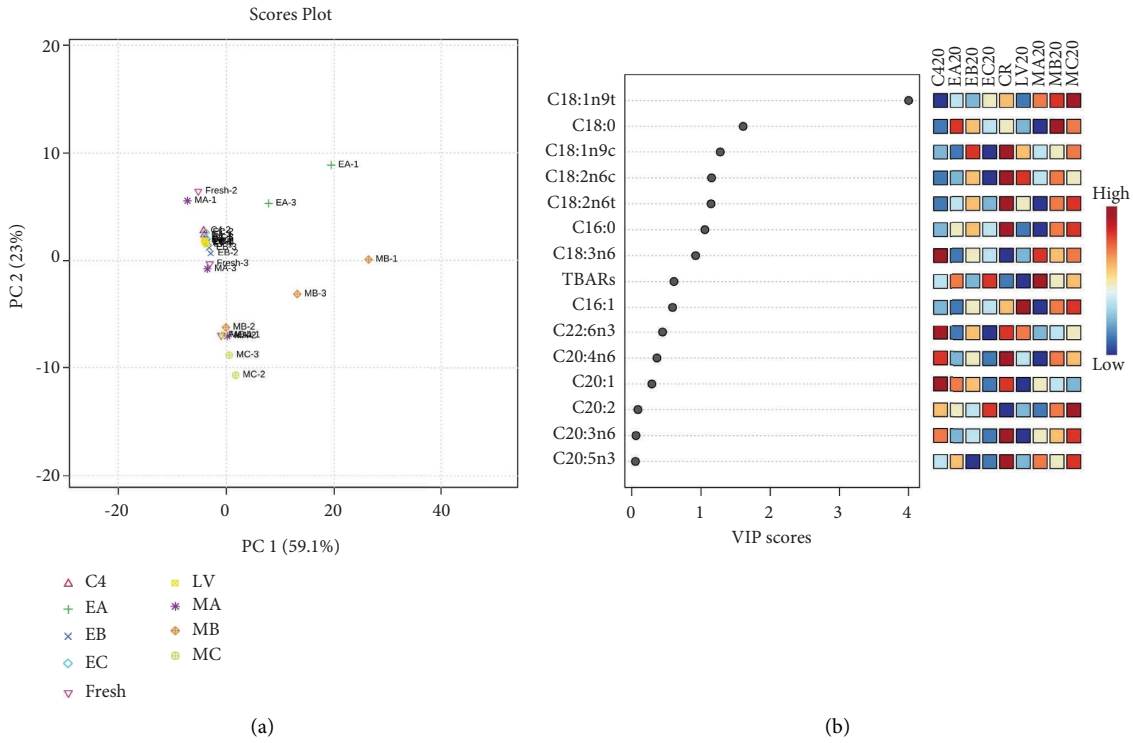

Figure 6: PCA and PLS-DA of fatty acids in PM on the 20th day of chilled storage. (a) Principal component analysis (PCA); (b) variable importance projection (VIP) score of fatty acids in PM on the 20th day. The colored boxes on the right represent the relative concentrations of fatty acids on the 20th day. C4 (refrigerated storage only), MA (50% CO_2 + 50% N_2), MB (10% O_2 + 40% CO_2 + 50% N_2), MC (20% O_2 + 30% CO_2 + 50% N_2), EA (2 kGy), EB (4 kGy), EC (8 kGy), and LV (1.20 kV/m).

between the MB and MC groups. Notably, there was a significant difference in fatty acid composition between the MB, MC, and fresh groups ($p < 0.05$). Changes in carbon dioxide content may cause this phenomenon. To gain a better understanding of the differential fatty acid composition among different treatment conditions, PLS-DA was performed (Figure 6(b)). VIP ≥ 1 was a commonly used criterion for screening differential metabolites [39]. Six fatty acids showed significant differences during PM preservation, including oleic acid (C18:1n9c), linoleic acid (C18:2n6c), stearic acid (C18:0), palmitic acid (C16:0), elaidic acid (C18:1n9t), and linolelaidic acid (C18:2n6t). Both palmitic acid and stearic acid are saturated fatty acids, but they exhibit opposite properties within the organism. Stearic acid (C18:0) could reduce both cardiac and cancer risks in humans. However, palmitic acid has been associated with increased low-density lipoprotein cholesterol, which could increase the risk of developing cardiovascular disease (CVD) in humans [38]. Previous studies have shown that palmitic acid is the most abundant saturated fatty acid, which decreases with increasing storage time [40]. The C4, MA, and LV groups had the lowest palmitic acid relative content among the treatment groups. The relative content of palmitic acid was the highest in the EBI, MB, and MC groups. Oxygen in the MB and MC groups prompted the production of ATP in muscle cells [41], which provided energy for the beta-oxidation of fatty acids and might have increased the relative content of palmitic acid. The ability of EBI to attack the olefinic bond structure in fatty acids accelerates the lipid autoxidation reaction, which together with beta-oxidation might have increased the relative content of palmitic acid [42]. Cis fatty acids are often considered beneficial for normal metabolism in the body. Both oleic acid and linoleic acid are examples of cis-unsaturated fatty acids. Studies have shown that oleic acid in human alpha-lactalbumin made lethal to tumors (HAMLET) could induce apoptosis in tumor cells [43]. Linoleic acid is an essential omega-6 fatty acid that can be metabolized into EPA in the human body. Recent studies have indicated that EPA could influence signaling pathways related to certain diseases and improve human immune function [44]. The fresh group had the highest linoleic acid content but showed a decreasing trend during storage. This was related to the fact that PUFA was easily oxidized by enzymes or external factors (e.g., oxygen and irradiation) [45]. The LV group had the highest linoleic acid content among the treatment groups, followed by the MB group. LVEF was able to inhibit the production of ROS and reduce the oxidation of linoleic acid. The ester bond between glycerol molecules and fatty acid ester bonds can be hydrolyzed during storage to increase the fatty acid content [46]. Therefore, the linoleic acid content in the MA group was lower than that in the MB and MC groups, because oxygen might prompt the production of ATP, which provided energy for the hydrolysis of lipids [41]. However, the increase in oxygen content likewise accelerated the oxidation of linoleic acid, making the linoleic acid content of the MB

group higher than that of the MC group. Some studies have demonstrated a close association between trans-fatty acids and the occurrence of cancer and cardiovascular diseases [47]. Compared with the retention time of fatty acid methyl ester standards, linolelaidic acid (C18:2n6t) and elaidic acid (C18:1n9t) were considered trans-fatty acids. Among them, elaidic acid had the largest VIP value. The relative amount of elaidic acid was highest in the MB and MC groups, again probably due to the hydrolysis of lipids. A comprehensive evaluation of six different fatty acids showed that the group treated by LVEF had the highest fatty acid quality.

4. Conclusions

Under chilled conditions, PM inevitably underwent oxidation of proteins and lipids, leading to the deterioration of the meat. This paper explored the inhibition effect of nonthermal technologies on protein and lipid oxidation of PM. Compared with other nonthermal technologies, LVEF could better stabilize the color and reduce the water loss of PM. During chilled storage, groups treated with LVEF had better tenderness than the other groups. Moreover, LVEF could reduce the oxidation of proteins by inhibiting the increase in carbonyl concentrations and decreasing the sulfhydryl concentrations of PM. The LVEF treatment avoided the degradation and cross-linking of the main proteins in the PM. The results of lipid oxidation showed that LVEF was more effective than MAP and EBI in inhibiting the increase in TBAR levels. Fatty acid analysis showed that the fatty acids of the samples treated with LVEF were similar to those of the fresh samples. The concentrations of the six differential fatty acids in the LVEF-treated group were beneficial to human health. In conclusion, the LVEF treated (1.20 kV/m) under chilled storage could reduce protein and lipid oxidation of PM, maintaining the functional and structural stability of proteins and lipids and inhibiting the rapid deterioration of PM quality. This study provided the basis for the industrial application of LVEF to maintain quality stability during PM chilled storage.

Data Availability

The data used to support the findings of this study are available from the corresponding authors upon reasonable request.

Conflicts of Interest

The authors declare that they have no conflicts of interest.

Authors' Contributions

Xiao-Yang Tong curated the data, designed the methodology, and wrote the original draft. Yi Zhang curated the data, designed the methodology, and wrote the review. Jin-Xin Pang designed the methodology, validated the data, and visualized the data. Bao-Lin Liu investigated the data, provided software, validated the data, and visualized the data. Eric Biron designed the methodology, validated the data, and visualized the data. Md R. T. Rahman investigated the data and provided software. Yong-Jin Qiao acquired funding and provided resources. Qi-Jie Bing designed the methodology and validated the data. Xu-Ying Gao administered the project and provided resources.

Acknowledgments

The authors express their deep thanks to the Shanghai Utility Pigeon Research System, the Shanghai Agricultural Products Preservation and Processing Engineering Technology Research Center, and the Shanghai Agricultural Products Preservation and Processing Professional Technical Service Platform, for supporting this research. This study did not use any AI software to prepare the manuscript. This research was supported by the Shanghai Utility Pigeon Research System (grant no. 202212), the Shanghai Agricultural Products Preservation and Processing Engineering Technology Research Center (19 DZ2251600), and the Shanghai Agricultural Products Preservation and Processing Professional Technical Service Platform (21 DZ2292200).

References

[1] C. L. Jin, Y. A. He, S. G. Jiang et al., "Chemical composition of pigeon crop milk and factors affecting its production: a review," *Poultry Science*, vol. 102, no. 6, Article ID 102681, 2023.

[2] M. N. Lund, M. S. Hviid, and L. H. Skibsted, "The combined effect of antioxidants and modified atmosphere packaging on protein and lipid oxidation in beef patties during chill storage," *Meat Science*, vol. 76, no. 2, pp. 226–233, 2007.

[3] Y. L. Bao, E. Puolanne, and P. Ertbjerg, "Effect of oxygen concentration in modified atmosphere packaging on color and texture of beef patties cooked to different temperatures," *Meat Science*, vol. 121, pp. 189–195, 2016.

[4] E. Puolanne and M. Halonen, "Theoretical aspects of water-holding in meat," *Meat Science*, vol. 86, no. 1, pp. 151–165, 2010.

[5] W. Jia, Q. Shi, R. Zhang, L. Shi, and X. Chu, "Unraveling proteome changes of irradiated goat meat and its relationship to off-flavor analyzed by high-throughput proteomics analysis," *Food Chemistry*, vol. 337, Article ID 127806, 2021.

[6] Y. L. Bao and P. Ertbjerg, "Effects of protein oxidation on the texture and water-holding of meat: a review," *Critical Reviews in Food Science and Nutrition*, vol. 59, no. 22, pp. 3564–3578, 2019.

[7] X. G. Wu, Z. G. Zhang, Z. Y. He et al., "Effect of freeze-thaw cycles on the oxidation of protein and fat and its relationship with the formation of heterocyclic aromatic amines and advanced glycation end products in raw meat," *Molecules*, vol. 26, no. 5, p. 1264, 2021.

[8] M. Liu, A. M. Lampi, and P. Ertbjerg, "Unsaturated fat fraction from lard increases the oxidative stability of minced pork," *Meat Science*, vol. 143, pp. 87–92, 2018.

[9] F. F. Hu, S. Y. Qian, F. Huang, D. Han, X. Li, and C. H. Zhang, "Combined impacts of low voltage electrostatic field and high humidity assisted-thawing on quality of pork steaks," *LWT-Food Science & Technology*, vol. 150, Article ID 111987, 2021.

[10] Y. Xie, B. Chen, J. Guo et al., "Effects of low voltage electrostatic field on the microstructural damage and protein

structural changes in prepared beef steak during the freezing process," *Meat Science*, vol. 179, Article ID 108527, 2021.

[11] M. C. Zhang, Z. C. Jin, R. Guo, and D. Y. Liu, "The two-stage air thawing based on low voltage electric field (LVEF) can make the quality of thawed chicken breast close to that before freezing," *LWT-Food Science & Technology*, vol. 173, Article ID 114344, 2023.

[12] Y. Xie, K. Zhou, B. Chen et al., "Applying low voltage electrostatic field in the freezing process of beef steak reduced the loss of juiciness and textural properties," *Innovative Food Science & Emerging Technologies*, vol. 68, Article ID 102600, 2021.

[13] J. Wyrwisz, M. Moczkowska, M. Kurek, A. Stelmasiak, A. Półtorak, and A. Wierzbicka, "Influence of 21days of vacuum-aging on color, bloom development, and WBSF of beef semimembranosus," *Meat Science*, vol. 122, pp. 48–54, 2016.

[14] S. J. Li, X. Guo, Y. Shen, J. Pan, and X. Dong, "Effects of oxygen concentrations in modified atmosphere packaging on pork quality and protein oxidation," *Meat Science*, vol. 189, Article ID 108826, 2022.

[15] C. Wang, H. Wang, X. Li, and C. H. Zhang, "Effects of oxygen concentration in modified atmosphere packaging on water holding capacity of pork steaks," *Meat Science*, vol. 148, pp. 189–197, 2019.

[16] K. Hirasaka, S. Saito, S. Yamaguchi et al., "Dietary supplementation with isoflavones prevents muscle wasting in Tumor-Bearing mice," *Journal of Nutritional Science and Vitaminology*, vol. 62, no. 3, pp. 178–184, 2016.

[17] J. Torten and J. R. Whitaker, "Evaluation of the biuret and dye-binding methods for protein determination in meats," *Journal of Food Science*, vol. 29, no. 2, pp. 168–174, 1964.

[18] Y. Y. Liu, L. T. Zhang, S. Gao et al., "Effect of protein oxidation in meat and exudates on the water holding capacity in bighead carp (Hypophthalmichthys nobilis) subjected to frozen storage," *Food Chemistry*, vol. 370, Article ID 131079, 2022.

[19] Y. H. Jo, K. A. An, M. S. Arshad, and J. H. Kwon, "Effects of e-beam irradiation on amino acids, fatty acids, and volatiles of smoked duck meat during storage," *Innovative Food Science & Emerging Technologies*, vol. 47, pp. 101–109, 2018.

[20] M. L. Henriott, N. J. Herrera, F. A. Ribeiro et al., "Impact of myoglobin oxygenation state prior to frozen storage on color stability of thawed beef steaks through retail display," *Meat Science*, vol. 170, Article ID 108232, 2020.

[21] Y. H. Kim, J. T. Keeton, S. B. Smith, J. E. Maxim, H. S. Yang, and J. W. Savell, "Evaluation of antioxidant capacity and colour stability of calcium lactate enhancement on fresh beef under highly oxidising conditions," *Food Chemistry*, vol. 115, no. 1, pp. 272–278, 2009.

[22] M. C. Zhang, X. F. Xia, Q. Liu, Q. Chen, and B. H. Kong, "Changes in microstructure, quality and water distribution of porcine longissimus muscles subjected to ultrasound-assisted immersion freezing during frozen storage," *Meat Science*, vol. 151, pp. 24–32, 2019.

[23] E. Huff-Lonergan and S. M. Lonergan, "Mechanisms of water-holding capacity of meat: the role of postmortem biochemical and structural changes," *Meat Science*, vol. 71, no. 1, pp. 194–204, 2005.

[24] Z. Derakhshan, G. Oliveri Conti, A. Heydari et al., "Survey on the effects of electron beam irradiation on chemical quality and sensory properties on quail meat," *Food and Chemical Toxicology*, vol. 112, pp. 416–420, 2018.

[25] Y. J. Kim, J. H. Song, D. Lee, S. H. Um, and S. H. Bhang, "Suppressing cancer by damaging cancer cell DNA using LED irradiation," *Journal of Photochemistry and Photobiology B: Biology*, vol. 243, Article ID 112714, 2023.

[26] B. M. Nyaisaba, X. X. Liu, S. C. Zhu et al., "Effect of hydroxyl-radical on the biochemical properties and structure of myofibrillar protein from Alaska pollock (*Theragra chalcogramma*)," *LWT-Food Science & Technology*, vol. 106, pp. 15–21, 2019.

[27] C. Faustman, Q. Sun, R. Mancini, and S. P. Suman, "Myoglobin and lipid oxidation interactions: mechanistic bases and control," *Meat Science*, vol. 86, no. 1, pp. 86–94, 2010.

[28] W. Z. Huo, R. Ye, Y. C. Shao, H. T. Wang, and W. J. Lu, "Insight into the mechanism of CO_2 to initiate and regulate ethanol-driven chain elongation by microbial community and metabolic analysis," *Journal of Environmental Chemical Engineering*, vol. 11, no. 5, Article ID 110537, 2023.

[29] M. Giladi, Y. Porat, A. Blatt et al., "Microbial growth inhibition by alternating electric fields," *Antimicrobial Agents and Chemotherapy*, vol. 52, no. 10, pp. 3517–3522, 2008.

[30] Y. Q. Shen, X. X. Guo, X. P. Li et al., "Effect of cooking temperatures on meat quality, protein carbonylation and protein cross-linking of beef packed in high oxygen atmosphere," *LWT-Food Science & Technology*, vol. 154, Article ID 112633, 2022.

[31] Y. Feng and H. O. Hultin, "Effect of pH on the rheological and structural properties of gels of water-washed Chicken-Breast Muscle at physiological ionic strength," *Journal of Agricultural and Food Chemistry*, vol. 49, no. 8, pp. 3927–3935, 2001.

[32] M. N. Lund, M. Heinonen, C. P. Baron, and M. Estévez, "Protein oxidation in muscle foods: a review," *Molecular Nutrition & Food Research*, vol. 55, no. 1, pp. 83–95, 2011.

[33] K. Limpisophon, H. Iguchi, M. Tanaka et al., "Cryoprotective effect of gelatin hydrolysate from shark skin on denaturation of frozen surimi compared with that from bovine skin," *Fisheries Science*, vol. 81, no. 2, pp. 383–392, 2015.

[34] M. Nikoo, S. Benjakul, and K. Rahmanifarah, "Hydrolysates from marine sources as cryoprotective substances in seafoods and seafood products," *Trends in Food Science & Technology*, vol. 57, pp. 40–51, 2016.

[35] Y. Q. Li, B. H. Kong, X. F. Xia, Q. Liu, and P. J. Li, "Inhibition of frozen storage-induced oxidation and structural changes in myofibril of common carp (*<scp>C</scp>yprinus carpio*) surimi by cryoprotectant and hydrolysed whey protein addition," *International Journal of Food Science and Technology*, vol. 48, no. 9, pp. 1916–1923, 2013.

[36] G. Liu and Y. L. Xiong, "Electrophoretic pattern, thermal denaturation, and in vitro digestibility of oxidized myosin," *Journal of Agricultural and Food Chemistry*, vol. 48, no. 3, pp. 624–630, 2000.

[37] B. Zhang, Y. Liu, H. H. Peng, Y. K. Lin, and K. Cai, "Effects of ginger essential oil on physicochemical and structural properties of agar-sodium alginate bilayer film and its application to beef refrigeration," *Meat Science*, vol. 198, Article ID 109051, 2023.

[38] T. Uushona, O. C. Chikwanha, C. L. F. Katiyatiya, P. E. Strydom, and C. Mapiye, "Fatty acid and oxidative shelf-life profiles of meat from lambs fed finisher diets containing Acacia mearnsii leaf-meal," *Meat Science*, vol. 201, Article ID 109190, 2023.

[39] Y. Ma, Y. F. Gao, Y. J. Xu et al., "Microbiota dynamics and volatile metabolite generation during sausage fermentation," *Food Chemistry*, vol. 423, Article ID 136297, 2023.

[40] D. Chaula, C. Jacobsen, H. S. Laswai et al., "Changes in fatty acids during storage of artisanal-processed freshwater

sardines (Rastrineobola argentea)," *Food Science and Nutrition*, vol. 11, no. 6, pp. 3040–3047, 2023.

[41] O. Savu and M. Militaru, "The intrinsec and extrinsec factors affecting the quality of chicken meat and their implications in food safety area," *Revista Romana de Medicina Veterinara*, vol. 24, no. 4, pp. 105–118, 2014.

[42] X. Huang and D. U. Ahn, "Lipid oxidation and its implications to meat quality and human health," *Food Science and Biotechnology*, vol. 28, no. 5, pp. 1275–1285, 2019.

[43] K. E. Chetta, M. Forconi, D. A. Newton, C. L. Wagner, and J. E. Baatz, "HAMLET in human milk is resistant to digestion and carries essential free long chain polyunsaturated fatty acids and oleic acid," *Food Chemistry*, vol. 427, Article ID 136752, 2023.

[44] M. Zhang, W. B. Lu, H. C. Yang et al., "Lipidomics study on the molecular changes of eicosapentaenoic and docosahexaenoic acyl structured glycerides during enzyme-catalysis and chemocatalysis," *LWT-Food Science & Technology*, vol. 148, Article ID 111815, 2021.

[45] M. Wereńska and A. Okruszek, "Impact of frozen storage on fatty acid profile in goose meat," *Poultry Science*, vol. 101, no. 12, Article ID 102213, 2022.

[46] J. S. Ribeiro, M. J. M. C. Santos, L. K. R. Silva et al., "Natural antioxidants used in meat products: a brief review," *Meat Science*, vol. 148, pp. 181–188, 2019.

[47] Y. P. Liang, D. Jiao, X. Du et al., "Effect of dietary agriophyllum squarrosum on average daily gain, meat quality and muscle fatty acids in growing Tan lambs," *Meat Science*, vol. 201, Article ID 109195, 2023.